IET Microwaves, Antennas & Propagation

Research Article

High-gain end-fire bow-tie antenna using artificial dielectric layers

ISSN 1751-8725
Received on 31st July 2014
Revised on 9th December 2014
Accepted on 7th April 2015
doi: 10.1049/iet-map.2014.0514
www.ietdl.org

Abdolmehdi Dadgarpour[1] ✉, *Behnam Zarghooni*[1], *Bal S. Virdee*[2], *Tayeb A. Denidni*[1]

[1]*INRS-EMT, University of Quebec, Montreal, QC, Canada*
[2]*Faculty of Computing, London Metropolitan University, London, UK*
✉ *E-mail: abdolmehdi.dadgarpour@emt.inrs.ca*

Abstract: This study presents a high-gain bow-tie antenna for applications in next generation base-stations operating from 2.5 to 3.9 GHz. The proposed structure consists of three circular sector patches that are attached laterally to the microstrip feed-line, which is etched on both sides of the common dielectric substrate to create symmetrical bow-tie antenna. By loading the antenna with a 2×5 array of enhanced end-coupled split-ring (EECSR) unit-cells results in significant enhancement in the antenna gain performance. This is because the EECSR unit-cells behave as parasitic radiators, which is analogous to Yagi–Uda antennas. The EECSR unit-cells provide a medium of high effective permittivity that effectively reduces the spacing between parasitic directors. As a consequence, a compact and miniature structure is achieved compared with conventional quasi-Yagi–Uda planar designs. The dimension of EECSR unit-cell is 33×36 mm^2 with inter-element spacing of $0.075\lambda_0$ at 3.5 GHz. A prototype of the antenna was fabricated and its performance was measured to validate the simulation results. The measured peak gain of the antenna with 4×5 array of EECSR is 12.65 dBi at 3.73 GHz, constituting a peak gain enhancement of 7.45 dBi in the Worldwide Interoperability for Microwave Access band compared with an equivalent conventional bow-tie antenna.

1 Introduction

Wireless communication systems such as cellular base-stations need to have antennas that operate at the Worldwide Interoperability for Microwave Access (WiMAX) band with high-gain characteristics necessary for long range applications. Conventional base-station networks employ a 1×4 antenna array to enhance its gain. Quasi-Yagi–Uda planar antenna structures have been reported to be an appropriate configuration for such applications [1–3], and a number of investigations have been carried out recently to enhance the gain of quasi-Yagi–Uda antennas. For instance, in [4], a compact Yagi–Uda antenna is described that consists of a folded driven element, where the director and reflector elements are bow-tie monopole structures used to increase the antenna bandwidth and attain the self-impedance that is necessary to optimise the driving-point impedance and gain. The radiating elements are spaced by $0.053\lambda_0$ to give an absolute gain in the range of 8.8–9.5 dBi. In [5], a simple coplanar waveguide quasi-Yagi printed antenna has been reported, which provides a maximum gain of 7.4 dBi at 10 GHz. In [6], a frequency switchable printed Yagi–Uda dipole sub-array (1×4) exhibits a maximum gain of 11.9 dBi at 3.4 GHz. However, the antenna is bulky and has dimensions of $238 \times 105 \times 62.4$ mm^3. Kramer *et al.* [7] have proposed a vertical multilayer stacked Yagi antenna working at the industrial, scientific and medical band of 5.8 GHz with a measured gain of 11 dBi. In fact, this antenna comprises of five circle-shaped patch directors with $0.28\lambda_0$ spacing between the radiators. The largest dimension of the antenna is its height, which is $1.16\lambda_0$ at 5.8 GHz. Another technique described in [8] uses zero-index metamaterial (ZIM) unit-cell as an electric-field coupled resonator to realise low refractive index for enhancing the antenna gain. Although this technique provides a gain enhancement of 6.43 dBi using three layers of ZIM unit-cells, the height of the proposed structure in the direction of propagation (broadside) is about $1.01\lambda_0$ at 10.6 GHz, which makes the structure too bulky. Alhalabi and Rebeiz [9] have proposed a high-gain Yagi–Uda antenna operating in the frequency range of 22–26 GHz using five directors with inter-element spacing $0.7\lambda_0$ at 24 GHz, which results in a measured gain of 9–11 dBi. However, the distance between the directors and the dipole in the end-fire direction is $0.96\lambda_0$ at 24 GHz. In addition, the measured side-lobe level in *H*-plane is around −4 dB with respect to the main beam at 25 GHz, which is unacceptable for most practical purposes.

This paper presents a high-gain planar bow-tie antenna that uses a unique technique to enhance its gain performance. The proposed antenna consists of periodic bow-tie radiators similar to that presented in [10]. However, it includes a 2×5 array of enhanced end-coupled split-ring (EECSR) unit-cells located symmetrically in the *H*-plane (*yz*-plane) and along the direction of the main beam. The EECSR unit-cells with inter-element spacing of $0.075\lambda_0$ between radiators behave as an artificial dielectric medium with a significantly higher effective permittivity. In this structure, the EECSR array also acts as parasitic elements. The measured peak gain of the proposed antenna using EECSR arrays is 12.65 dBi at 3.73 GHz. Conventional quasi-Yagi bow-tie antennas using five director elements, which are spaced by $0.3–0.4\lambda_0$ and arranged in the *E*-plane, provide gain improvement of 6 dBi; however, they are substantially larger $1.53\lambda_o \times 1.19\lambda_o \times 0.70\lambda_o$ [7]. In this paper, we propose a bow-tie antenna using artificial dielectric layers loaded with 4×5 array of EECSRs that provide a peak gain enhancement of 7.45 dBi and smaller dimensions ($1.27\lambda_o \times 0.53\lambda_o \times 0.42\lambda_o$) compared with the quasi-Yagi and patch antenna reported in [7–9].

2 Design principle

A conventional planar quasi-Yagi antenna consists of a driven element backed by a reflector and a number of parasitic elements as directors in the direction of the main beam. The space (d) between directors can be determined by

$$d = \frac{\lambda_0}{4} \times \frac{1}{\sqrt{\varepsilon_r}} \tag{1}$$

where λ_0 is the wavelength of the signal in free space, and ε_r is the dielectric constant of the antenna substrate. The above equation

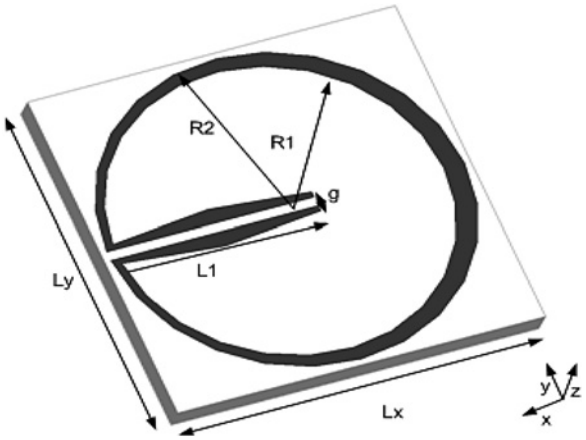

Fig. 1 *Geometry of the proposed EECSR unit-cell*

indicates that if the dielectric constant is increased, the director spacing can be reduced, which results in miniaturisation of the antenna structure.

To realise a high effective permittivity, we have modified the circular patch described in [7] by using an EECSR resonator structure shown in Fig. 1. In this structure, the *E*-field is polarised along the plane of the unit-cell and the *H*-field is polarised normal to the ring in order to induce current on the periphery of ring. The proposed unit-cell was constructed on a Rogers RT/duroid 5880 substrate with the thickness of $h = 1.575$ mm, relative permittivity of 2.2 and loss tangent of 0.0009. The dimensions of the unit-cell are: $R_1 = 8.1$ mm, $R_2 = 8.6$ mm, $L_1 = 9.7$ mm, $L_x = 18$ mm, $L_y = 18$ mm and $g = 0.5$ mm.

The intrinsic electrical parameters of the proposed unit-cell such as effective permittivity and permeability were acquired using a standard extraction algorithm described in [11], which is based on the *S*-parameters calculated using the Ansoft high-frequency structural simulator (HFSS). This involved assigning the perfect electric conducting and the perfect magnetic conducting boundary conditions in the *yz*-plane and *xy*-plane to the EECSR structure in Fig. 1. The extracted effective permittivity and permeability of the proposed EECSR unit-cell and a reference circular patch are shown in Fig. 2. To better understand the behaviour of the EECSR structure, the effective permittivities of the EECSR with various radii were computed. The results shown in Fig. 2 indicate a shift in the peak effective permittivity from around 3.6–3.9 GHz when the radius of the unit-cell is decreased from 8 to 7 mm. The upward frequency shift is used to increase the antenna gain bandwidth in Section 6. The simulation result confirms that the EECSR structure behaves like an artificial dielectric substrate whose effective permittivity is substantially higher than the substrate especially in the frequency range of 3.4–3.6 GHz.

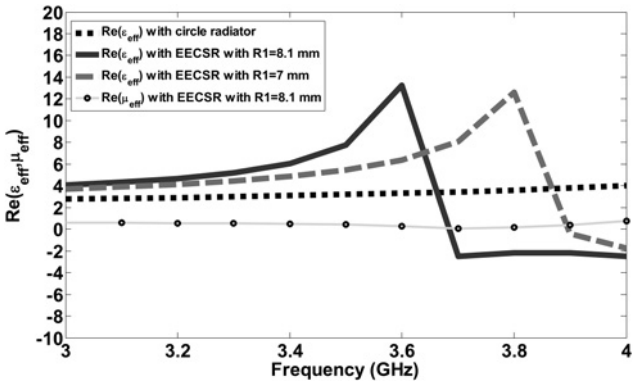

Fig. 2 *Effective permittivity and permeability of the proposed EECSR unit-cell compared with a reference circular patch*

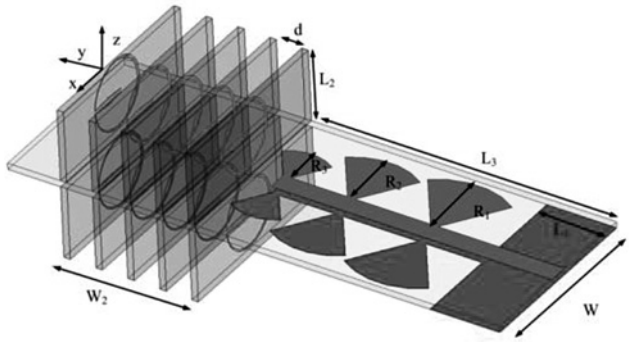

Fig. 3 *Three-dimensional structural view of the proposed antenna comprising of bow-tie antenna loaded with 2 × 5 array of EECSR unit-cells*

The results indicate that by applying the EECSR unit-cell on the Rogers 5880 substrate leads to a high effective permittivity medium, for example, at 3.5 GHz the permittivity is 8 for a unit-cell with a radius of 8.1 mm. As a consequence, according to (1), the spacing (d) between the radiators can be reduced. In the proposed design, the distance is 7.58 mm. Furthermore, it will be shown in the next section that the antenna gain can be enhanced by stacking a number of EECSR layers without significantly affecting the size of the antenna.

3 Bow-tie antenna with EECSR unit-cell layers

The proposed antenna consists of two sections, where the first section is a modified form of the bow-tie antenna presented in [10] which is designed to operate in the frequency range of 2.5–3.9 GHz. The antenna essentially consists of three circular sector patches that are attached laterally to the microstrip feed-line, which is constructed on both sides of the dielectric substrate to create symmetrical bow-tie radiators, as shown in Fig. 3. The length of each patch section is a quarter-guided wavelength, and the three patches are designed to resonate at 2.5, 3.1 and 3.8 GHz. The flare angle of each patch radiator was selected to be 75° to maximise the impedance matching of the antenna. The second part consists of a 2 × 5 array of EECSR unit-cell layers, symmetrically mounted normal to the plane of the bow-tie radiators, as shown in Fig. 3, to enhance the antenna gain analogous to Yagi–Uda antennas. The length of each unit-cell along the z-direction is $L_2 = 0.21\lambda_0$ (18 mm) at 3.5 GHz. The arrangement of the two unit-cells along the z-direction act as directors with dimension of $2 \times L_2 \simeq 0.42\lambda_0$. In the design, the initial gap between the radiators (d) was deduced to be 7.58 mm at 3.5 GHz using (1). The dimensions of the structure are: $R_1 = 8$ mm, $R_2 = 8.7$ mm, $R_3 = 5$ mm, $L_1 = 17.5$ mm, $L_2 = 18$ mm, $L_3 = 75$ mm, $W = 45$ mm, $d = 6.5$ mm and $W_2 = 33$ mm.

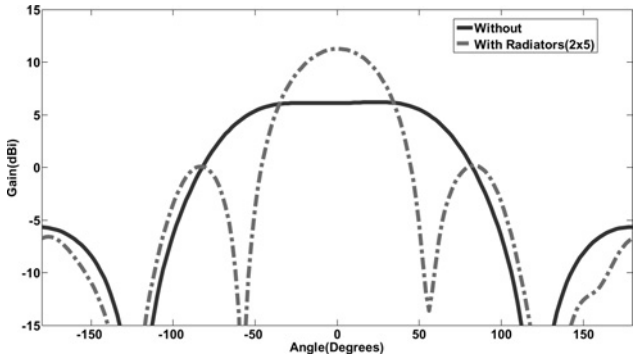

Fig. 4 *Radiation pattern of the proposed antenna in the H-plane (yz) with and without EECSR loading (2 × 5 array) at 3.5 GHz*

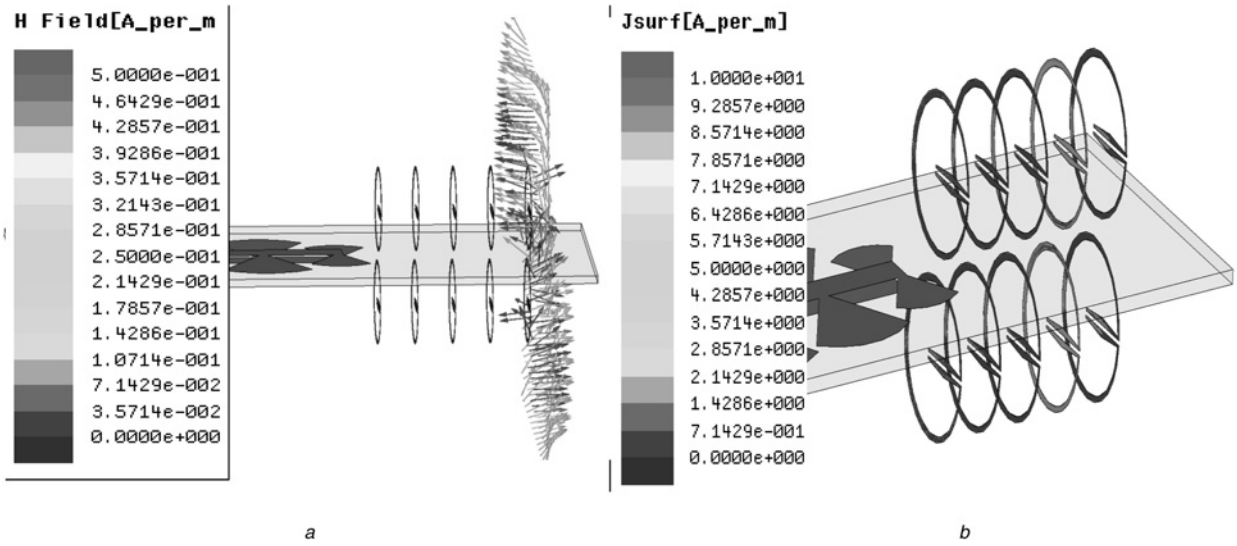

Fig. 5 *Magnetic field of the antenna and its effect on the EECSR arrays*

a Distribution of *H*-field
b Surface current distribution on the EECSR array at 3.5 GHz

Using the optimisation tool in Ansoft HFSS version 14, the optimum spacing between the radiators was found to be 6.5 mm ($0.075\lambda_0$) at 3.5 GHz. The numerical investigation using HFSS showed that by incorporating a 2×5 array of EECSR along the *y*-direction results in enhancement of gain by 5.7 dBi at 3.5 GHz, as shown in Fig. 4, which is higher than the one reported in [7]. Furthermore, using a stack of five parasitic elements with overall dimensions of 33×36 mm^2 makes the proposed antenna significantly smaller than the structure described in [7–9].The periodicity of the unit-cell is essentially along the *y*-direction. Other examples where a single metamaterial unit-cell has been employed to modify the characteristics of the antenna are reported in [12, 13].

Figs. 5*a* and *b* show the magnetic field of the antenna and its effect on the EECSR arrays. If we consider the antenna as a transverse electromagnetic source, the magnetic field should be in end-fire direction (+*y*) which is perpendicular to the EECSR plane as shown in Fig. 5*a*. As a result, it induces a current distribution on the EECSR elements as shown in Fig. 5*b*. This indicates that the EECSR array acts as parasitic element that affects the radiation from the bow-tie antenna and contributes towards the antenna's gain enhancement in Fig. 4.

4 Parametric study

This section describes the results of the investigation undertaken to determine how different number of EECSR unit-cells affect the gain performance of the proposed antenna in the *H*-plane (*yz*). Fig. 6 shows the radiation pattern in the *H*-plane at 3.5 GHz with different numbers of EECSR unit-cell along the *y*-axis. These results indicate that a larger gain enhancement is achieved when the number of the directors is increased. As described in the previous section, each director is in fact a 2×1 array of the EECSR unit-cells, which is mounted symmetrically on the both sides of the common substrate. According to Fig. 6, when just one director is used along the *y*-direction, the gain enhancement in the *H*-plane is 1.5 dBi. By increasing the number of the aforementioned directors to three, leads to a gain enhancement of 4.5 dBi. A five-fold increase in directors results in a gain improvement of 5.7 dBi, with a total gain of 11.2 dBi.

The effect of the spacing between the directors on the antenna gain was also investigated. Fig. 7 shows that if the spacing between the directors (d) is increased, then there is a corresponding increase in the antenna gain. For instance, if $d = 6.5$ mm ($0.075\lambda_0$ at 3.5 GHz), the resulting gain is 11.2 dBi. Moreover, it is observed from the results that if the gap is increased from $0.07\lambda_0$ to $0.11\lambda_0$, the resulting gain enhancement is about 0.6 dBi. Hence, the gap size between the directors used here was made to be $0.07\lambda_0$ to realise a compact antenna structure with a high-gain performance.

To show the capability of the proposed antenna in polarisation-diversity applications, we used it in a dual-polarised configuration as shown in Fig. 8*a*.The radiation pattern of the resultant system when one port is exited and the other port is terminated is shown in Fig. 8*b*. The maximum gain observed is 11.6 dBi at 3.6 GHz.

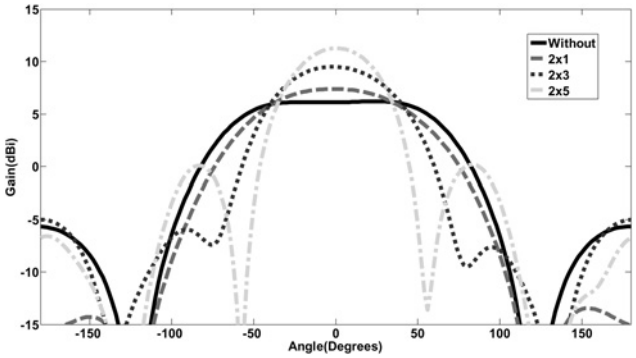

Fig. 6 *Radiation pattern of proposed antenna in the H-plane with different number of EECSR unit-cell layer loading in the y-direction at 3.5 GHz*

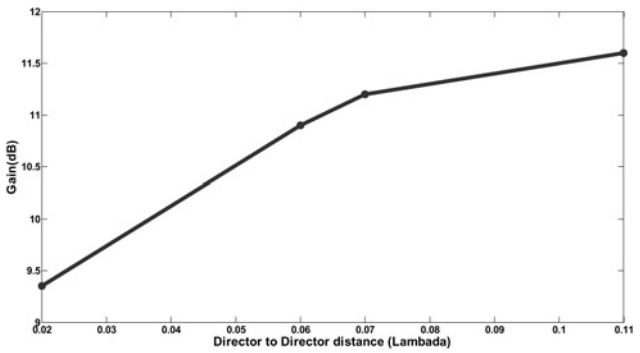

Fig. 7 *Antenna gain as a function of the distance between radiators at 3.5 GHz*

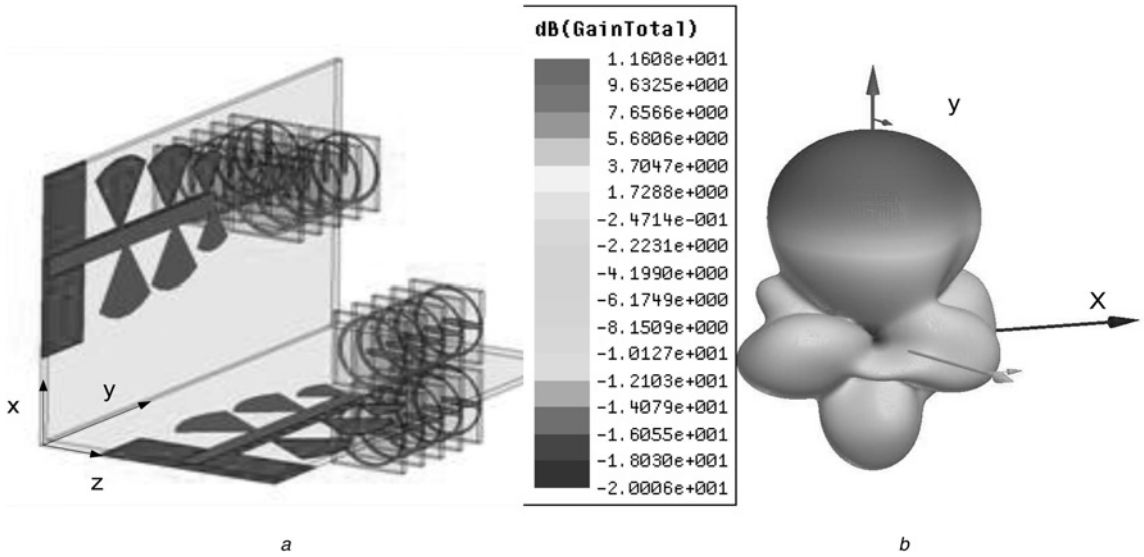

Fig. 8 *Capability of the proposed antenna in polarisation-diversity applications*

a Configuration of dual-polarised high-gain EECSR antenna
b Radiation pattern of the antenna when excited at 3.5 GHz

5 Experimental results

The simulation results of the proposed high-gain antenna with the embedded parasitic elements to form the 2×5 array of EECSR unit-cell layers were validated by fabricating a prototype of the antenna and measuring its performance. The measured reflection coefficient and its photograph are shown in Figs. 9 and 10. These results show that the EECSR layers have insignificant impact on the reflection coefficient of the antenna, which is better than −10 dB in the WiMAX band. The measured radiation patterns of the proposed antenna with the EECSR array in the *H*- and *E*-planes at 3.5 GHz are plotted in Fig. 11. The correlation between the simulated and measured results is good. The SLL of the antenna in the *H*-plane is <−11 dB, and the front to back radiation in both planes is better than −18 dB, which is much better than the proposed Yagi–Uda antenna in [9]. Measurements of the peak gain of the bow-tie antenna with and without EECSR array was carried out using the gain-comparison method with a known standard horn antenna at different frequencies within the WiMAX band. The measured peak gain, as shown in Fig. 12, rises from 9.7 dBi at 3.4 GHz to 10.9 dBi at 3.6 GHz. There is a 5.7 dBi gain improvement over the bow-tie antenna without EECSR layers at 3.6 GHz. The discrepancies between the simulation and measured results are attributed to inaccurate simulation models, fabrication tolerance and the losses resulting from the dielectric, surface waves and the connector effect.

6 Antenna gain bandwidth

In this section, a study on the gain bandwidth performance of the EECSR array is presented. The results of this study are given in Fig. 12. The gain of the proposed EECSR array antenna is compared when replaced with dielectric slabs of $\varepsilon_r = 6$ and 10.2. The results show that the 2×5 EECSR array provides a significantly higher gain performance than the dielectric slabs; however, the EECSR antenna suffers from a narrow gain bandwidth performance. The gain of the EECSR 2×5 array varies between 8.36 and 10.97 dB over a frequency range of 3.2–3.6 GHz. Over the same frequency range of 3.2–3.6 GHz, the slab with $\varepsilon_r = 6$ exhibits a gain that varies between 7.0 and 7.76 dB, and the slab with $\varepsilon_r = 10.2$ has a gain that varies between 7.45 and 8.36 dB.

To improve the gain bandwidth performance, the 2×5 array of EECSR unit-cells with inner radius $R_1 = 7$ mm was integrated with another 2×5 array with inner radius $R_1 = 8.1$ mm to create a 4×5

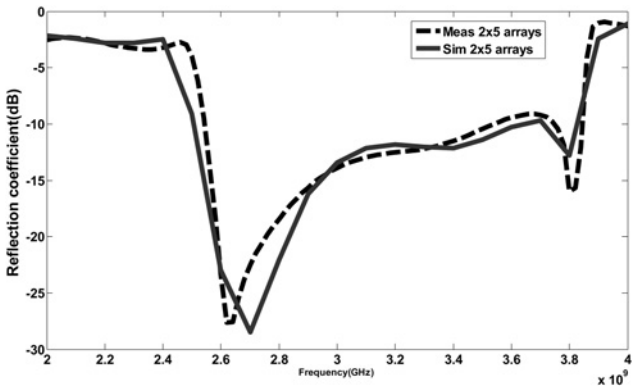

Fig. 9 *Simulated and measured reflection coefficients of antenna with and without the EECSR*

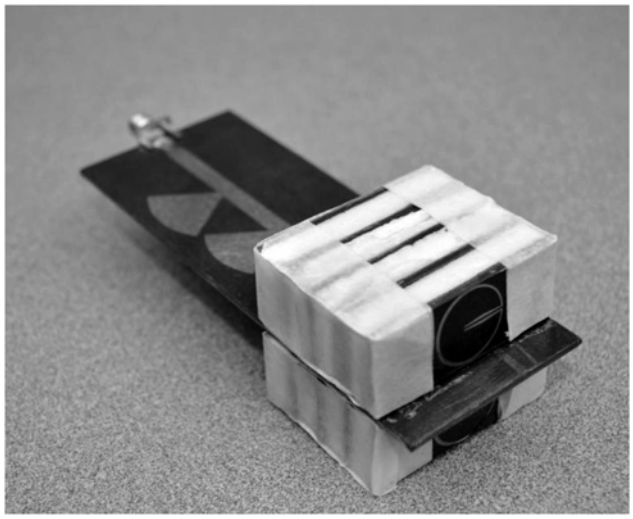

Fig. 10 *Photograph of the fabricated prototype antenna*

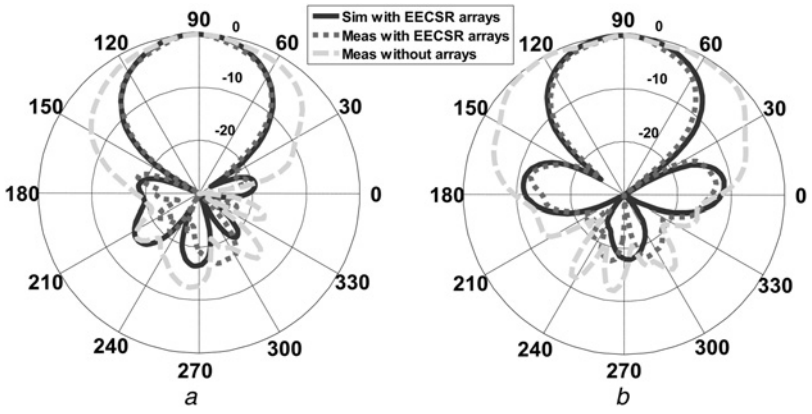

Fig. 11 *Normalised simulated and measured radiation patterns of proposed antenna with EECSR array at 3.5 GHz*

a *E*-plane (*xy*)
b *H*-plane (*yz*)

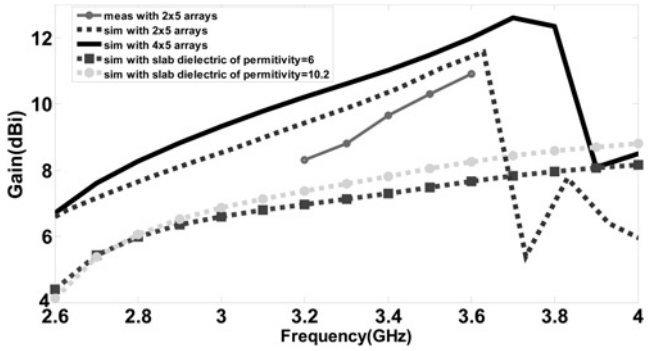

Fig. 12 *Simulated and measured peak gains*

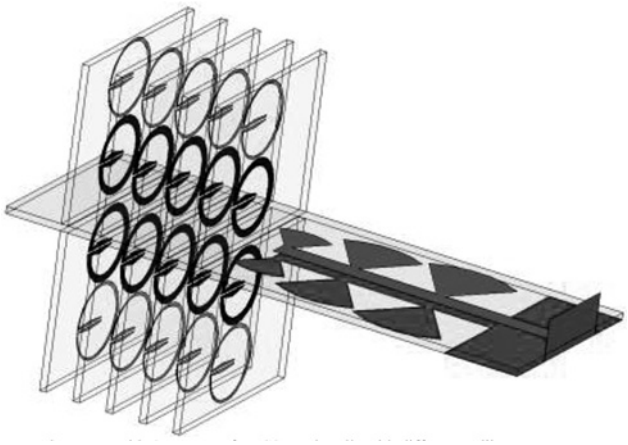

Fig. 13 *Proposed antenna with 4 × 5 array of EECSR unit-cells with different radii*

Table 1 Comparison of the proposed antenna with other works

Ref.	Average gain, dBi	Bandwidth, GHz	Dimensions
[5]	5.4	8.0–12.0	$0.97\lambda_0 \times 0.64\lambda_0$ at 10 GHz
[6]	10.3	2.4–3.58	$2.70\lambda_0 \times 1.19\lambda_0 \times 0.70\lambda_0$ at 3.4 GHz
[7]	10	5.8	$1.53\lambda_0 \times 1.19\lambda_0 \times 0.70\lambda_0$ at 5.8 GHz
[8]	11.9	10.6	$1.50\lambda_0 \times 1.50\lambda_0 \times 0.90\lambda_0$ at 10 GHz
this work	10.0	3.15–3.9	$1.27\lambda_0 \times 0.53\lambda_0 \times 0.42\lambda_0$ at 3.5 GHz

array shown in Fig. 13. The effect of the EECSR unit-cell with inner radius R_1 was discussed in Section 2. The proposed EECSR unit-cell with the inner radius of $R_1 = 7$ mm provides a high permittivity over the frequency range of 3.65–3.85 GHz, as shown in Fig. 2. The high permittivity leads to a high refractive index as $n = (\mu\varepsilon)^{1/2}$. Snell's law is given by

$$n_{\text{mtm}} \sin\theta_1 = n_0 \sin\theta_2 \tag{2}$$

where n_{mtm} is the refractive index of EECSR unit-cell, and n_0 is the refractive index of air region. Equation (2) indicates that increasing the refractive index of the metamaterial region will result in a larger refracting angle (θ_2). By employing high-permittivity provided by EECSR unit-cells with the radius of 7 mm, the aperture size of the antenna is effectively enhanced over the whole frequency range of 3.65–3.85 GHz. This is the mechanism that is employed here to improve the gain bandwidth performance of the antenna. The gain bandwidth performance of the antenna with 4 × 5 array, in Fig. 12, shows the antenna provides a gain better than 10 dBi over 3.15–3.9 GHz, but the gain is significantly enhanced in the range of 3.6–3.9 GHz with a maximum gain of 12.65 dBi at 3.73 GHz. Table 1 shows the advantage of the proposed gain enhancement technique compared with other conventional methods [5–8]. The reflection coefficient of the antenna with 4 × 5 array of EECSR unit-cells with different radii is shown in Fig. 14 which demonstrates that the impedance bandwidth is also increased by 150 MHz from 3.85 to 4 GHz.

The *E*- and *H*-plane radiation patterns of the antenna for the 4 × 5 array of EECSR at 3.8 GHz are plotted in Fig. 15.

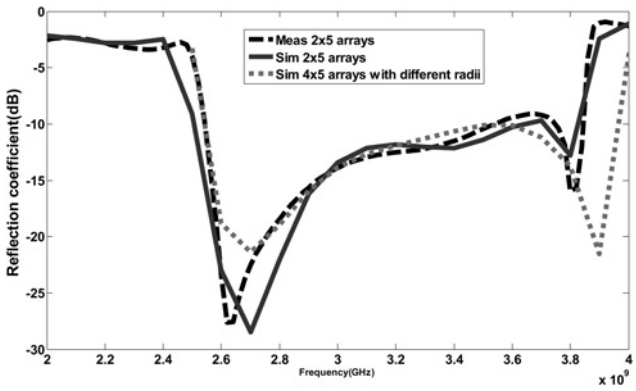

Fig. 14 *Comparison of the reflection coefficient (S_{11}) response of EECSR array with different radii ($R_1 = 8.1$ and 7 mm)*

IET Microw. Antennas Propag., 2015, Vol. 9, Iss. 12, pp. 1254–1259

Fig. 15 *E- and H-plane radiation patterns of proposed antenna with 4 × 5 array of EECSR at 3.8 GHz*

7 Conclusion

A unique gain enhancement technique has been described for a bow-tie antenna structure designed to operate in the WiMAX frequency band (2.5–3.9 GHz). The proposed structure consists of an artificial dielectric structure in the form of a 4×5 array of EECSR radiator unit-cells oriented normal to the direction of the main beam to provide a high effective permittivity medium for the radiation emanating from the bow-tie antenna. The EECSR array essentially behaves as a parasitic director. The peak gain of the proposed antenna is 12 dBi at 3.85 GHz, and the measured gain of the antenna without EECSR loading is only 5.2 dBi, resulting in gain enhancement of 6.8 dBi at 3.85 GHz. In addition, the antenna reflection coefficient is better than -10 dB in the WiMAX band from 2.5 to 3.9 GHz with inclusion of the parasitic elements. Owing to its high gain and compact size, the proposed technique and antenna structure can be applied in future WiMAX base-stations for mobile communication systems.

8 References

1 Cheng, D.K., Chen, C.A.: 'Optimum element spacing for Yagi–Uda arrays', *IEEE Trans. Antennas Propag.*, 1973, **AP-21**, (5), pp. 615–623

2 Nikolic, N., Weily, A.R.: 'Compact E-band planar quasi-Yagi antenna with folded dipole driver', *IET Microw. Antennas Propag.*, 2009, **4**, (11), pp. 1728–1734

3 Kan, H., Abbosh, A., Waterhouse, R., Bialkowski, M.: 'Compact broadband coplanar waveguide-fed curved quasi-Yagi antenna', *IET Microw. Antennas Propag.*, 2007, **1**, (3), pp. 572–574

4 Arceo, D., Balanis, C.A.: 'Design methodology for a reactively loaded Yagi–Uda antenna', *IEEE Antenna Wirel. Propag. Lett.*, 2012, **11**, pp. 795–798

5 Kan, H.K., Waterhouse, R.B., Abbosh, A.M., Bialkowski, M.E.: 'Simple broadband planar CPW-FED quasi Yagi antenna', *IEEE Antenna Wirel. Propag. Lett.*, 2012, **6**, pp. 18–20

6 Cai, Y., Guo, Y.J., Qin, P.-Y.: 'Frequency switchable printed Yagi–Uda dipole sub-array for base station antennas', *IEEE Trans. Antennas Propag.*, 2012, **60**, (3), pp. 1639–1642

7 Kramer, O., Djerafi, T., Wu, K.: 'Vertically multilayer-stacked Yagi antenna with single and dual polarizations', *IEEE Trans. Antennas Propag.*, 2010, **60**, (3), pp. 1022–1030

8 Li, D., Szabó, Z., Qing, X., Li, E.-P., Chen, Z.: 'A high gain antenna with an optimized metamaterial inspired superstrate', *IEEE Trans. Antennas Propag.*, 2012, **60**, (12), pp. 6018–6023

9 Alhalabi, R.A., Rebeiz, G.M.: 'High-gain Yagi–Uda antennas for millimeter-wave switched-beam systems', *IEEE Trans. Antennas Propag.*, 2009, **57**, (11), pp. 3672–3676

10 Qu, S.-W., Li, J.-L., Xue, Q., Chan, C.-H.: 'Wideband periodic end-fire antenna with bowtie dipoles', *IEEE Antennas Wirel. Propag. Lett.*, 2008, **7**, pp. 314–317

11 Chen, X., Grzegorczyk, T.M., Wu, B.I., Pacheco, J.Jr., Kong, J.A.: 'Robust method to retrieve the constitutive effective parameters of metamaterials', *Phys. Rev. Lett., E*, 2004, **70**, p. 16608

12 Ketzaki, D.A., Yioultsis, T.V.: 'Metamaterial-based design of planar compact MIMO monopoles', *IEEE Trans. Antennas Propag.*, 2013, **61**, (5), pp. 2758–2766

13 Cao, W., Xiang, Y., Zhang, B., Liu, A., Yu, T., Guo, D.: 'A low-cost compact patch antenna with beam steering based on CSRR-loaded ground', *IEEE Antennas Wirel. Propag. Lett.*, 2011, **10**, pp. 1520–1523